BIOCELL
2021 45(2): 259-266

Tech Science Press

Tritrichomonas foetus: New structures by high-resolution scanning helium ion microscopy

Marlene BENCHIMOL[1,3,*]; Abigail MIRANDA-MAGALHÃES[2]; Antonio PEREIRA-NEVES[2]; Wanderley De SOUZA[3]

[1] Universidade do Grande Rio, Duque de Caxias, 25071-202, Rio de Janeiro
[2] Departamento de Microbiologia, Laboratório de Biologia Celular de Patógenos, Fiocruz, Instituto Aggeu Magalhães, Recife, 52060-269, Brazil
[3] Universidade Federal do Rio de Janeiro, Instituto de Biofísica Carlos Chagas Filho, Laboratório de Ultraestrutura Celular Hertha Meyer Instituto Nacional de Ciência e Tecnologia (INBEB) and Centro Nacional de Biologia Estrutural e Bioimagens (CENABIO), Rio de Janeiro, 21941-902, Brazil

Key words: Nanotubes, Microvesicles, Surface specializations

Abstract: Helium ion scanning microscopy (HIM) is a novel high-resolution scanning microscopy technique that uses helium ions instead of electrons to form images of the highest quality and resolution, providing a sub-nanometer resolution sputter uncoated biological cell. Here, we took advantage of HIM to explore the cell surface of *Tritrichomonas foetus*, a protist parasite of cattle that provokes hard infection and abortion in cows. We describe thin protrusions, like nanotubes described in other cells, with different sizes (27 nm to 81 nm in thickness) and various lengths (from 73 nm to 2 μm), as well bulbous structures either budding from the cell surface or present in the extremities of some protrusions. The flagella also presented these thin protrusions and different protein decoration, similar to those previously described using freeze-fracture techniques. Nanotubes between two cells were also seen, and their role in infection is discussed. The cell surface was also examined and showed several pits indicative of endocytic activity and other types of arrays of particles. These observations were confirmed using Scanning Electron Microscopy (SEM), negative staining, and conventional thin sectioning for observation by transmission electron microscopy. Our findings provide new and relevant information that may contribute to a better understanding of protozoan biology and its interaction with mammalian cells.

Introduction

The flagellated protist *Tritrichomonas foetus* is a parasite that causes bovine trichomonosis, a significant sexually transmitted disease in cattle. *T. foetus* has a worldwide distribution and causes substantial economic losses and health problems since trichomonosis in cows ranges from slight infections to severe manifestations of disease such as vaginitis, placentitis, and pyometra. It can result in infertility, early embryonic death, or abortion in cattle. *T. foetus* can also colonize the large intestine of cats, leading to feline tritrichomonosis, or live as a commensal in the nasal mucosa of pigs (Dąbrowska *et al.*, 2020). The trichomonad pathogenesis mechanisms are multifactorial. Because of economic and veterinary consequences, basic research is imperative to understand this pathogen better and search for other intervention strategies.

*Address correspondence to: Marlene Benchimol, marlenebenchimol@gmail.com
Received: 11 October 2020; Accepted: 23 December 2020

Studies carried out in several pathogenic protists have shown that the most important antigenic molecules are located on the cell surface (Reviews in De Souza, 1995; Mucci *et al.*, 2017). Therefore, it is important to know the structural organization of these eukaryotic microorganisms' surface in more detail. Recent studies have provided evidence that *Trichomonas vaginalis* release extracellular vesicles through its surface. These vesicles contain many molecules involved in several biological processes, such as tetraspanins and small RNAs (Twu *et al.*, 2013; Artuyants *et al.*, 2020). These vesicles were isolated, labeled, and then incubated in the presence of epithelial cells. It was shown that they interfere with several interleukins' secretions and can even be transferred for other parasite strains, interfering with some functions (Olmos-Ortiz *et al.*, 2017).

It has recently been published that several cell types present thin membrane protrusions, which have received several distinct names such as cytonemes, membrane extensions, tunneling nanotubes-like protrusions (TNT), and cellular bridges, specialized filopodia, and signaling filopodia (Reviewed in Yamashita *et al.*, 2018). It has been

Doi: 10.32604/biocell.2021.014599

proposed that these protrusions would play some role in a novel mechanism of direct intercellular communication. Concerning parasitic protozoa, (Szempruch *et al.*, 2016) demonstrated that membranous nanotubes are formed from the flagellar membrane at the posterior region of African trypanosomes and that subsequently, vesicles are released by the process of strangulation of the tubules.

Microscopy, especially Scanning Electron Microscopy (SEM), has been used to analyze many cell types' surfaces, including pathogenic protozoa (Sant'Anna *et al.*, 2005; De Souza and Attias, 2018). More recently, important improvements in the SEM allowed us to obtain high-resolution images in the range of 0.8 to 1 nm. These improvements included (a) The use of field emission guns that generate beams with a small diameter but with variable energy, (b) The use of highly sensitive secondary and backscattered electron detectors well positioned in relation to the sample, among other factors (Review in De Souza and Attias, 2018). Also, a new microscope, known as Helium Ion Microscopy (HIM), was developed. It is based on the use of ions rather than electron beams. This equipment allows the obtainment of high-quality images that can reach a sub-nanometer resolution. Such high resolution is due to the beam's high brightness using a tiny probe size and the relatively short wavelength of He^+, enabling the beam to be focused on dimensions until 0.3 nm. In the present work, we used high-resolution SEM and HIM as well as transmission electron microscopy of thin sections and negatively stained cells to analyze in more detail the surface of *T. foetus*. Images were obtained, revealing new surface structures. Here, we describe the presence of thin and long protrusions from the cell surface and flagella of *T. foetus*, which have not been described before in this parasite.

Materials and Methods

Parasites cultures

The K strain of *Tritrichomonas foetus* was isolated by Dr. H. Guida (Embrapa, Rio de Janeiro, Brazil) from the urogenital tract of a bull. It was cultured in Diamond's Trypticase-yeast extract-maltose (TYM) medium supplemented with 10% horse serum at 37°C for 30 h, which corresponds to the logarithmic growth phase.

Transmission electron microscopy

Ultra-thin sections: Parasites (1×10^6) were fixed in 2.5% glutaraldehyde in 0.1 M cacodylate buffer, pH 7.2. Cells were post-fixed in 1% OsO_4 and 0.8% potassium ferricyanide, dehydrated in acetone, and embedded in Epon (Polybed 812). Ultra-thin sections were harvested on 300-mesh copper grids, stained with 5% uranyl acetate and 1% lead citrate, and observed with an FEI Tecnai Spirit transmission electron microscope. The images were acquired with a CCD camera system (MegaView G2, Olympus, Germany).

Negative staining: Parasites were settled onto positively charged Alcian blue-coated carbon film nickel grids (Labhart and Koller, 1981) for 5 min at 37°C. Next, cells were fixed in 2.5% glutaraldehyde in PEME (100 mM PIPES pH 6.9, 1 mM $MgSO_4$, 2 mM EGTA, 0.1 mM EDTA) for 1h at room temperature. Parasites were washed with water and negatively stained with 1% aurothioglucose (UPS Reference Standard) in water for 5 s. The grids were then air-dried and observed as described above.

Scanning electron microscopy

Conventional scanning electron microscopy (SEM) was performed for comparison purposes. Samples were washed three times in warm PBS (pH 7.2) and then fixed in 2.5% glutaraldehyde in 0.1 M cacodylate buffer, pH 7.2. Cells were then post-fixed for 20 min in 1% OsO_4, dehydrated in ethanol and critical point dried with liquid CO_2. The dried cells were coated with 20 nm–25 nm thick of gold-palladium and then observed with a JEOL 5600 scanning electron microscope.

Helium ion microscopy

The samples were prepared similarly to the samples used for SEM, except for the ion-sputter step (i.e., the cells were not coated). The images were captured using a 28 kV ion energy and a working distance of 8.5 mm, Blanker current of 1.6 pA, on an ORION Helium Ion Microscope (Carl Zeiss, Oberkochen, Germany). No conductive coatings were applied to the samples before imaging to preserve the sample surface information. The images were formed from the detection of induced secondary electrons and constructed as a 2048-2240-pixel array.

Samples were transferred into the HIM via a load-lock system and were maintained at a vacuum of $2–3 \times 10^{-7}$ Torr during the imaging session. Charge control was maintained using a low energy electron flood gun, which was applied in a temporally interlaced fashion with the imaging beam. Images were formed by collecting the secondary electrons elicited by the interaction between the helium ion beam and the sample with an Everhart-Thornley Microchannel plate (Everhart and Thronely, 1960) Wideband detector for micro-ampere low energy electron currents. This detector is also widely used in SEM and consists of a scintillator placed inside a Faraday cage, that draws the elicited low voltage secondary electrons towards it. The resulting photons are collected, turned into electrons, and amplified by a photomultiplier tube (PMT). The PMT signal is then digitized using an A/D converter and displayed as a grey value in each pixel of the resulting image. The scanning of the helium ion beam and the image's formation are synchronized so that there is a corresponding signal or grey value in the resulting image for any given coordinate. No post-processing procedures were applied to the digital images besides brightness and contrast adjustment. The image signal was acquired in a line-averaging mode, with either 32 or 64 lines integrated into each line in the final image. Charge neutralization was applied after each line pass of the beam.

Results

As previously described by conventional preparation for scanning electron microscopy, *T. foetus* presents a teardrop-shaped body with three anterior flagella and one recurrent flagellum. Its surface and flagellum are usually described as displaying a smooth surface. However, when high-resolution

HIM is used, this morphology can be better visualized using cells that were not previously coated with a metal layer, a great advantage of this microscope. With this approach, it was possible to visualize both the cell body's cell surface and flagella with high visibility (Figs. 1–5). We analyzed at least 100 cells for each image obtained in this work, and about 50% of the cells exhibited the mentioned structures. The following surface structures were visualized. First, many surface protrusions with variable shapes, length, and thickness/diameter (Figs. 1–5). These include (a) Surface projections with a mean diameter of 70 nm (Fig. 1a). Some of them were straightforward, ending freely, with a length that may reach 4 μm (Fig. 1). Others seemed to connect adjacent cells (Fig. 1b).

Still, others showed a non-straight orientation, displaying a curved appearance. They can be seen at the anterior region, in between the anterior flagella (Figs. 1a–1b and 2a), in the tip of flagella (Fig. 5c), and in the cell body, especially near the area of attachment of the recurrent flagellum to the cell body (Figs. 2b and 4). The high resolution provided by HIM also revealed a background full of material probably secreted by the protozoan (Figs. 2a–2b). Spherical vesicles closely associated with the cell surface with a diameter varying from 130 nm to 200 nm and slightly thicker projections with a mean diameter of 240 nm were also seen (Fig. 2b).

Several protrusions were observed (Figs. 5a–5d). In the posterior end of the cell body, a thin protrusion with 68 nm thickness and 490 nm length was observed (Fig. 5b). Protrusions can even curl up in the flagellum, as shown in Fig. 5c. Besides, protrusions with a length of 600 nm show a different pattern, originating small vesicles with a mean diameter of 100 nm (Fig. 5d). Most of these structures could also be visualized after careful examination of the cells using conventional SEM (Fig. 5c). However, their thickness was slightly higher, probably due to the 10 nm–20 nm-thick layer of gold usually used to avoid charge problems during the interaction of the electrons with the cell surface.

Flagella

The anterior flagella were imaged with remarkable preservation and clarity (Figs. 1, 2, 4, and 6), presenting several decoration spots that appear as rounded depressions (Figs. 4–5a) with a mean diameter of 12 nm–15 nm. About 2–60 spots were seen per square micrometer. In the region where the three anterior flagella (AF) emerge, thin tubular protrusions measuring between 37 nm to 58 nm were seen (Figs. 1, 2a–2b, and 5a). We also noticed bulbous protrusions at the end of some tubular extensions measuring between 52 nm to 64 nm (Figs. 1b, 2, and 5).

Recurrent flagellum

In the region of the undulating membrane and the recurrent flagellum, thin nanotubes measuring between 40 nm to 53 nm and bulbous protrusions on the recurrent flagellum measuring 82 nm to 130 nm were seen (Figs. 1a and 2b). Links between the plasma membrane and the recurrent flagellum (Fig. 2b), and tubular nanotubes and bulbous structures with different sizes, from 130 to 160 nm, were observed. A unique decoration was seen along the recurrent flagellum both on the undulating membrane and plasma membrane's cell surface. It is essential to mention that the undulating membrane exhibited a decoration and several pits (Figs. 4a–4b). Ribbon-like arrays of particles were seen along the length of the recurrent flagellum (Fig. 4a).

Negative staining

TEM of entire cells negatively stained cells confirmed and extended the results obtained by HIM. We found thin nanotubular extensions protruding from the tip (Fig. 5d) or along the anterior flagella (Figs. 2c–2d). These nanotubes exhibited a range size from 39 nm to 88 nm in thickness and a variable-length from 0.3 μm to 6 μm. In some cells, the tubular/bulbous protrusions were observed to shed from the flagellar tips (Fig. 5d), suggesting that these structures could be released from the flagellar membrane into the extracellular milieu. Bulbous protrusions measuring between 84 nm to 460 nm in diameter were also found in the tubular extension's root and tip regions (Figs. 2c–2d).

Ultrathin sections

Ultrathin sections of the flagella revealed that the thin protrusions are continuous with the flagella surface (Fig. 6), indicating that the nanotubes can be originated directly from

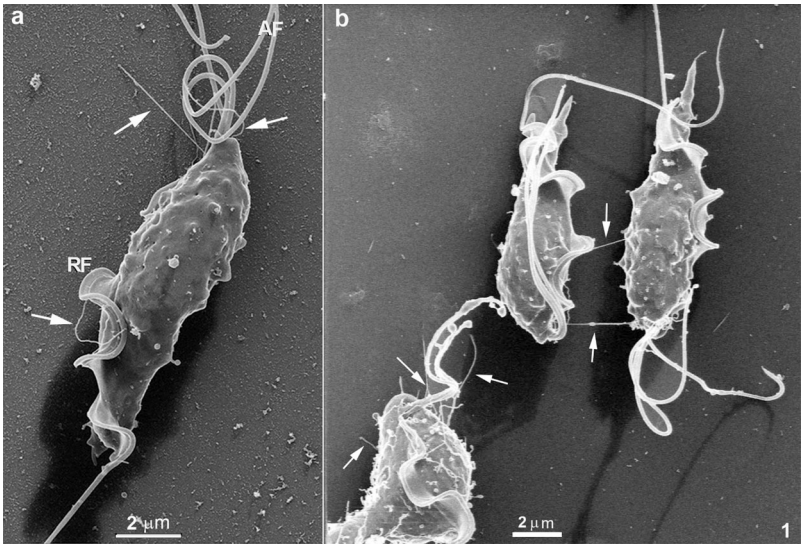

FIGURE 1. Scanning Helium Ion microscopy of *T. foetus*.
The cells are teardrop-shaped, presenting three anterior flagella (AF) and one recurrent flagellum (RF). HIM reveals thin membrane protrusions (arrows) measuring between 60 nm to 80 nm in thickness. Notice in (b) that two cells are connected through thin nanotubes measuring about 27 nm (arrows). In the cell seen on the left corner, it is possible to note several surface projections, both bulbous and tubular thin protrusions (arrows), measuring 73 and 100 nm, respectively. Bars: 2 μm.

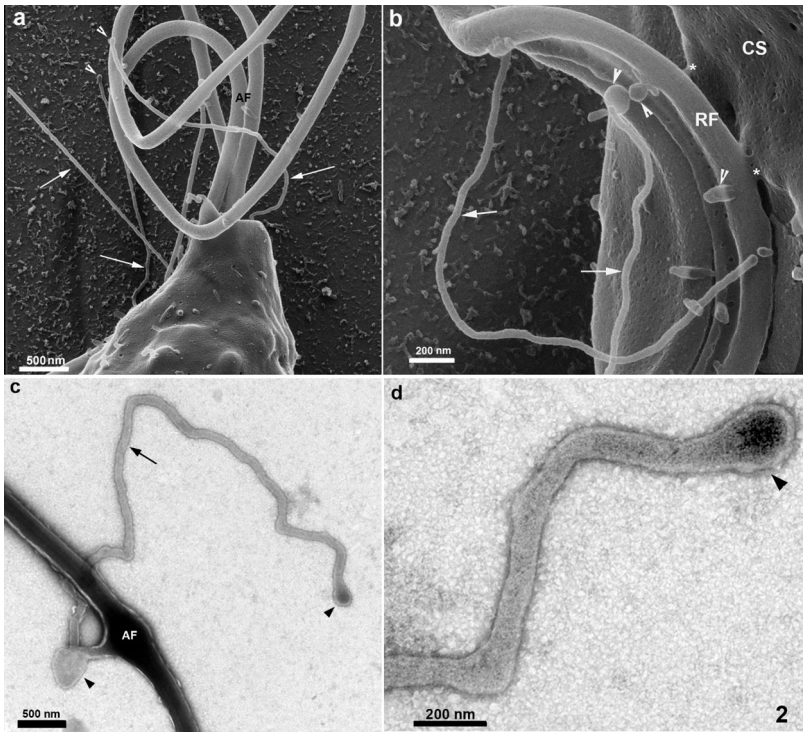

FIGURE 2. Scanning Helium Ion microscopy of the anterior region of *T. foetus*.
(a) It is the region where the three anterior flagella (AF) emerge. Thin tubular protrusions (arrows) measuring between 37 nm to 58 nm are seen. Notice that there are bulbous protrusions in the ends of some tubular extensions (arrowheads) measuring between 52 nm to 64 nm. The background reveals different materials eliminated by the cells. Small spots corresponding to endocytosis are found over the cell membrane. (b) Region of the undulating membrane and the recurrent flagellum. Thin nanotubes (arrows) measuring between 40 nm to 53 nm and bulbous protrusions on the recurrent flagellum (RF) measuring 82 nm to 130 nm are seen. Notice that several openings are distributed over the cell surface (CS), measuring 15 nm to 20 nm. Links between the plasma membrane and the recurrent flagellum is noted (asterisk). The background appears full of material eliminated by the cell. (c–d) Representative TEM images of an anterior flagellum (AF) negatively stained with 1% aurothioglucose. (c) General view of a nanotubular structure (arrow) protruding from the flagellar surface, measuring approximately 70 nm thickness and 6.8 μm length. Bulbous protrusions (arrowheads) are seen in the tubular extension's root and tip regions, measuring about 460 nm and 180 nm, respectively. (d) Close view of the tip region showing the bulbous protrusion (arrowhead). Bars: a and c, 500 nm; b and d, 200 nm.

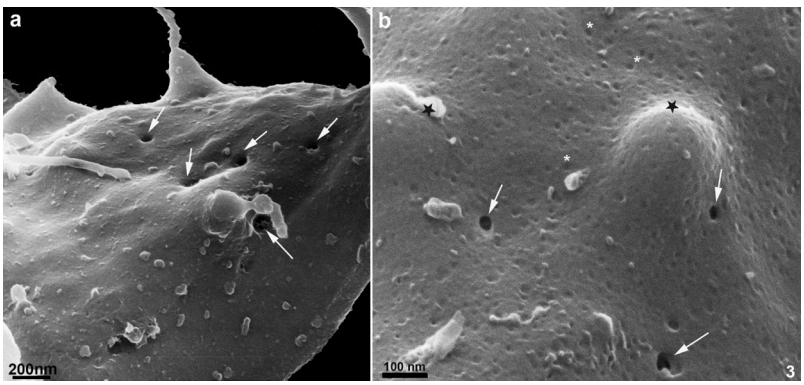

FIGURE 3. Scanning Helium Ion microscopy of the cell surface of *T. foetus*.
(a–b) Close view of cell surface where endocytic pits are depicted (arrows) with a size average of 65 nm and several spots suggestive of cell surface exocytose or endocytic activity (asterisks), measuring about 20 nm. Note in (b) two large protrusions in protuberances (stars) with approximately 200 nm. Bars: a, 200 nm; b, 100 nm.

a lateral extension of the flagellar membrane. We also noticed that the flagellar membrane projections' lumen is electron-lucent (Fig. 6), similar to the extracellular vesicles' lumen.

Discussion

Studies carried out with several eukaryotic cells, including some pathogenic protozoa, have shown that examining the cell surface using new methodological approaches, most of the time, reveals new morphological details. Indeed, the cattle parasitic protozoan *Tritrichomonas foetus* has already been studied in some detail by conventional SEM and TEM electron microscopy, as well as by freeze-fracture and freeze-etching methods (Benchimol *et al.*, 1982; 1992). Since conventional SEM uses a metal coat of different thicknesses, the actual cell surface is partially covered by metallization. Depending on the thickness used, many cell details are covered and lost.

Here we present new and relevant information on this protozoan's cell surface organization using initially high-resolution Helium Ion Microscopy. Several cell surface specializations could be seen using conventionally cultivated and fixed cells. However, it has been shown that HIM allows a

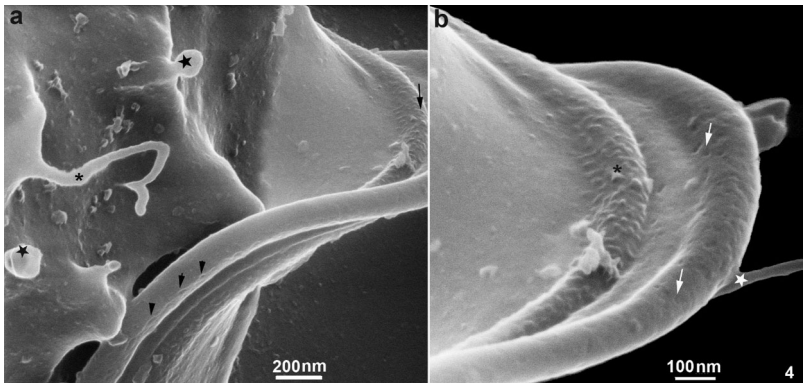

FIGURE 4. Scanning Helium Ion microscopy of the cell surface of *T. foetus*.
Region of adhesion of the recurrent flagellum forming the undulating membrane. (a) Tubular nanotubes (asterisk), bulbous structures (star) with different sizes (from 130 to 160 nm). Unique decoration is seen along the flagellum (arrowheads) and on the undulating membrane (arrows), as ribbon-like arrays of particles along the flagellum's length. (b) Details of the undulating membrane with a decoration (asterisk). Note that several pits are also observed (arrows). The star indicates a thin nanotube projecting from the undulating membrane. Bars: a, 200 nm; b, 100 nm.

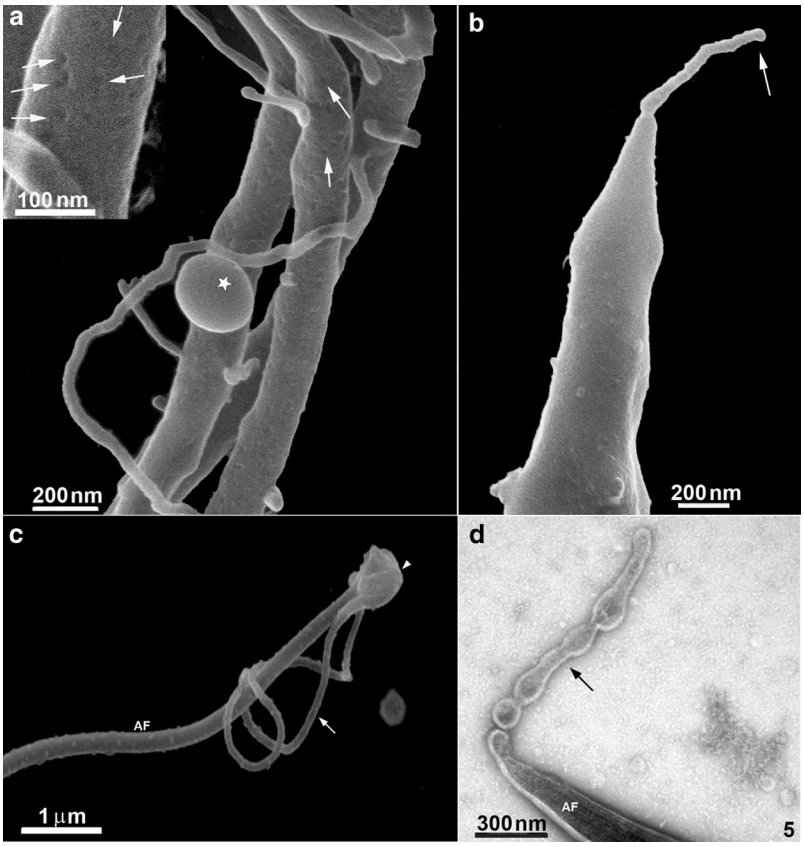

FIGURE 5. Scanning Helium Ion microscopy of the flagella surface of *T. foetus*.
(a) Notice the different sizes in the length of filamentous structures, which present a thickness of about 60 nm. Several pits are seen (arrows), which are better visualized in the inset. (b) Detail of the cell body posterior end where it is possible to note a thin protrusion with 68 nm thickness and 490 nm length. (c) Conventional SEM of an anterior flagellum (AF). Note a thin tubular extension (arrow) protruding from a bulbous structure (arrowhead) in the tip region. Measurements: thin extension: 91 nm thickness and 6.4 µm length; Bulbous structure: 750 nm thickness. (d) TEM of the tip region of an anterior flagellum (AF) negatively stained with 1% aurothioglucose. Notice a tubular/bulbous protrusion (arrow) shedding from the flagellum, measuring approximately 64 nm in the thinner region, 140 nm in the bulbous region, and 1 µm length. Bars: a, inset, 100 nm; a–b, 200 nm; c, 1µm; d, 300 nm.

resolution around three times higher than that provided by the best scanning electron microscopes. Also, it does not require a metal coating of the sample and allows a much higher depth of field (Reviewed in De Souza and Attias, 2018). Below, we will further discuss the main surfaces that could be visualized and, subsequently, confirmed using negative staining and thin sections.

Contrary to the prevalent idea that the surface of the protozoan is relatively smooth and homogenous. Our present observations revealed a myriad of nanometric surface projections whose function is not yet clear at this point. However, they may increase secretory activity and establish contact with neighbor cells, and we can speculate that *in vivo* probably with epithelial cells from the hosts.

The first structure to be mentioned comprises surface projections with a mean diameter of 70 nm that vary in length and shape. Based on their dimensions, they can be considered a member of the tunneling nanotube (TNT) family, most probably equivalent to structures previously designated as cytonemes, characterized by a diameter ranging from 50 to 200 nm (Reviewed in De Souza and Barrias, 2020). Our present observations show that these structures exist in *T. foetus* and can reach a length of up to 4 µm and probably more. Interestingly, some of these structures are straightforward, ending freely or apparently connecting the cells in the culture, as shown in Figs. 1 and 2, respectively. In some way, this structure resembles the

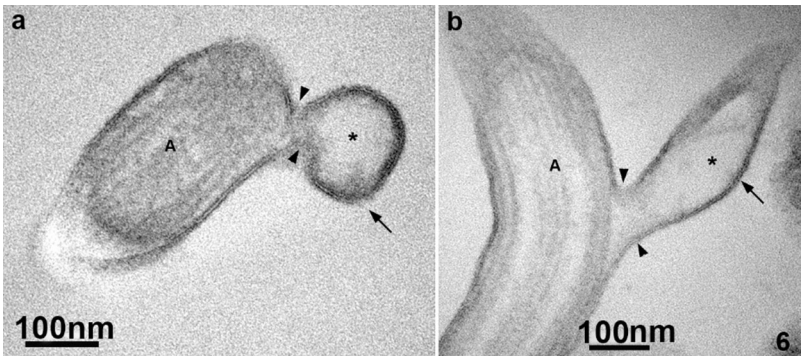

FIGURE 6. TEM of ultrathin sections of the anterior flagella of *T. foetus*.
(a) oblique-transversal, and (b) longitudinal views. Notice thin membrane projections (arrows) emerging from the flagella. The axoneme (A) is tightly surrounded by the flagellar membrane, which is continuous with the tubular protrusions (arrowheads). Observe that the protrusions' lumen (*) is electron lucent. Bars: 100 nm.

organization of some nanotubes found in the parasitophorous vacuole of cells infected with *Toxoplasma gondii*, where they connect the parasite surface with the membrane lining the vacuole (De Souza and Attias, 2015; 2018). We also observed other similar structures, but without a straight organization, displaying a highly curved appearance and emerging from different cell regions, including the flagella. It is important to point out that in a few cases, small ramifications from the main TNT could be noticed (see, for instance, Fig. 2a), and sometimes their end shows a spherical shape, with a mean diameter of 700 nm, suggesting a possible release of vesicles. These protrusions, which resemble the TNTs, have been considered an efficient mode of communication employed by many cell types. This mechanism was related to pathogenesis, including cancers and infections. In several diseases, cells may be physically connected utilizing the thin protrusions structures (either open-ended or close-ended) to send or receive various cargoes involved in disease progression (see Yamashita *et al.*, 2018 for a review). It is well established that most nanotubes and similar structures, such as filopodia, require the actin cytoskeleton and its regulators for their formation and function (Kornberg and Roy, 2014). However, the mechanisms that promote their formation are still under discussion (Delage *et al.*, 2016). Our present observations show the thin protrusions in contact between two cells, which might be suggesting a possible role for nanotubes in parasite-to-parasite communication.

Our results also suggest that the nanotubular structures could be released from flagella into the extracellular milieu. In this sense, some authors have reported such a process in the bloodstream African trypanosomes that constitutively shed membrane in the form of nanotubes, which are originated from the flagellar membrane, that subsequently dissociate into free extracellular vesicles (Szempruch *et al.*, 2016; Umaer *et al.*, 2018). In this case, the vesicles could be formed by a constriction of the tubes with subsequent release of vesicles, an idea supported by images such as those shown in Figs. 2a–2b, 4a, and 5d. Live-cell imaging experiments in other cells show that vesicles travel along these filopodia, further suggesting they allow cytoplasmic material transfer between linked cells. The thin protrusions have been considered conduits for signaling at a distance. Previous studies showed that signaling ligands were observed moving along nanotubes directly, further suggesting the involvement of these thin membrane protrusions in signal transduction (Hsiung *et al.*, 2005).

Additionally, further studies showed that cells in culture could exchange mitochondria and other organelles through larger nanotube-like communication between cells (Wang and Gerdes, 2015). One possibility that deserves further studies is that vesicles originated at the end, or even laterally, of the TNTs, are transferred from cell to cell, in some way establishing direct communication between cells. Studies carried out with *Trypanosoma cruzi* have indicated that transference of vesicles containing tRNA-derived small RNAs can be transferred from one parasite to the other, interfering with the process of metacyclogenesis (Garcia-Silva *et al.*, 2013).

Why were these nanotubular surface structures not visualized before? We have at least two explanations. First, because, as shown previously, they are extremely sensitive to mechanical stress and chemical fixation. Washing and centrifugation of the cells, a usual procedure during the preparation of cells in suspension for electron microscopy, may break the TNTs. Second, as previously discussed, the new generation of scanning microscopes with resolution better than 1 nm facilitates the visualization of such thin and delicate structures.

The second structure to be discussed comprises a series of vesicles associated with the protozoan surface that vary in size from 130 to 200 nm. Therefore, they can be included in designated as Extracellular Vesicles (EVs) (Witwer and Théry, 2019). Recent studies provided evidence for the release by *Trichomonas vaginalis* in the culture medium of vesicles with a diameter varying from 25 to 200 nm. They contain a heterogeneous population of small RNAs and many proteins (Twu *et al.*, 2013). These vesicles may correspond to those we observed associated with the protozoan surface in the present study. (Twu *et al.*, 2013) showed that they could be incorporated by epithelial cells and induce the production of IL6 and IL8, confirming the observation made by (Olmos-Ortiz *et al.*, 2017) for IL-6, IL-13, and IL-17. It is important to point out that the released vesicles may be transferred to other parasites and interfere with their ability to attach to epithelial cells *in vitro* (Twu *et al.*, 2013).

Further studies are necessary to establish these vesicles' biogenesis because they can represent either exosomes or ectosomes. Besides, we cannot exclude the possibility that some of them originate from the nanotubular structures discussed above. A third observation that deserves some discussion is the visualization for the first time using a scanning microscope of spots as rounded depressions on the anterior surface, but not of the recurrent flagella. Based on

the localization and the size, we consider that they may correspond to the rosettes first described using the freeze-fracture technique (Benchimol *et al*., 1982). Subsequently, using the quick frozen, freeze-fractured, deep-etching, and rotary replication technique there was shown that the rosettes protrude to the actual flagellar surface (Benchimol *et al*., 1992). This observation reinforces the high resolution provided by the HIM.

A fourth observation is related to the region of attachment of the recurrent flagellum to the protozoan body. We observed that this region is the focus of the emergence of TNTs and exhibited a decoration with several pits and ribbon-like arrays of particles seen along the length of the recurrent flagellum. The images obtained by HIM confirm previous observations made by freeze-fracture where ribbon-arrays of particles were observed, which confirms not only these special proteins arrangements but also the resolution provided by HIM, indicating that HIM has the potential to produce images of cells that surpass what is currently achievable with electron microscopy.

Few publications have applied HIM to the evaluation of uncoated biological samples. One beautiful work was reported by (Rice *et al*., 2013) in the rat kidney. In parasite protozoa, (Gadelha *et al*., 2015) published a piece of detailed and new information concerning the cytoskeleton of *Giardia intestinalis* using HIM with fascinating and unique results. In *Toxoplasma gondii*, De Souza and Attias (2015) described new features of the relationship between the parasite and the parasitophorous vacuole. In the present manuscript, we describe details of the *T. foetus* surface, including the presence of nanotubes that may connect a protozoan to each other. Taken together, we can conclude that the use of high-resolution scanning microscopy is a valuable tool to improve our knowledge of the structural organization of pathogenic protozoa.

Conclusion

New structures were observed with high-resolution scanning helium ion microscopy, which allows advances in the knowledge of the parasite *Tritrichomonas foetus* and opens new avenues for the understanding of the biology of this parasite.

Acknowledgement: The authors thank Endre Majorovits (Carl Zeiss, Oberkochen, Germany) for support with the Zeiss Orion microscope. We thank to Dr. Karina Saraiva and Dr. Cássia Docena from the Technological Platform Core of the Aggeu Magalhães Institute for their technical support.

Availability of Data and Materials: They are avaiable.

Author Contribution: Study conception and design: WS, APN. Data collection: MB, APN, AMM. Analysis and interpretation of results: WS, MB, APN. Draft manuscript preparation: WS, MB, APN. All authors reviewed the results and approved the final version of the manuscript.

Funding Statement: This work was supported by the Conselho Nacional de Desenvolvimento Cientifico e Tecnologico (CNPq), Programa de Excelência a Pesquisa/ Instituto Aggeu Magalhães (CNPq/PROEP-IAM grant: 400740/2019-2), Financiadora de Estudos e Projetos (FINEP), and Fundação Carlos Chagas Filho de Amparo à Pesquisa no Estado do Rio de Janeiro (FAPERJ).

Conflicts of Interest: The authors declare that they have no conflicts of interest to report regarding the present study.

References

Artuyants A, Campos TL, Rai AK, Johnson P, DUROS-Singorenko P, Phillips A, Simoes-Barbosa A (2020). Extracellular vesicles produced by the protozoan parasite *Trichomonas vaginalis* contain a preferential cargo of tRNA-derived small RNAs. *International Journal for Parasitology* **50**: 1145–1155. DOI 10.1016/j.ijpara.2020.07.003.

Benchimol M, Elias CA, De Souza W (1982). *Tritrichomonas foetus*: Fine structure of freeze-fractured membranes. *Journal of Protozoology* **29**: 348–353. DOI 10.1111/j.1550-7408.1982.tb05413.x.

Benchimol M, Kachar B, De Souza W (1992). Surface domains in the pathogenic protozoan *Tritrichomonas foetus*. *Journal of Protozoology* **39**: 480–484. DOI 10.1111/j.1550-7408.1992.tb04835.x.

Dąbrowska J, Keller I, Karamon J, Kochanowski M, Gottstein B, Cencek T, Frey CF, Müller N (2020). Whole genome sequencing of a feline strain of *Tritrichomonas foetus* reveals massive genetic differences to bovine and porcine isolates. *International Journal for Parasitology* **50**: 227–233. DOI 10.1016/j.ijpara.2019.12.007.

Delage E, Cervantes DC, Pénard E, Schmitt C, Syan S et al. (2016). Differential identity of filopodia and tunneling nanotubes revealed by the opposite functions of actin regulatory complexes. *Scientific Reports* **6**: 1007. DOI 10.1038/srep39632.

De Souza W (1995). Structural organization of the cell surface of pathogenic protozoa. *Micron* **26**: 405–430. DOI 10.1016/0968-4328(95)00010-0.

De Souza W, Attias M (2015). New views of *Toxoplasma gondii* parasitophorous vacuole as revealed by Helium Ion Microscopy (HIM). *Journal of Structural Biology* **191**: 76–85. DOI 10.1016/j.jsb.2015.05.003.

De Souza W, Attias M (2018). New advances in scanning microscopy and its application to study parasitic protozoa. *Experimental Parasitology* **190**: 10–33. DOI 10.1016/j.exppara.2018.04.018.

De Souza W, Barrias E (2020). Membrane-bound extracellular vesicles secreted by parasitic protozoa: Cellular structures involved in the communication between cells. *Parasitology Research* **119**: 2005–2023. DOI 10.1007/s00436-020-06691-7.

Everhart T, Thronely RFM (1960). Wide band detector for micro-ampere low energy electron currents. *Journal of Scientific and Industrial Research* **37**: 246–248.

Gadelha APR, Benchimol M, De Souza W (2015). Helium ion microscopy and ultra-high-resolution scanning electron microscopy analysis of membrane-extracted cells reveals novel characteristics of the cytoskeleton of *Giardia intestinalis*. *Journal of Structural Biology* **190**: 271–278. DOI 10.1016/j.jsb.2015.04.017.

Garcia-Silva MR, Cura das Neves RF, Cabrera-Cabrera F, Sanguinetti J, Medeiros LC, Robello C, Naya H, Fernandez-Galero T, Souto-Padron T, de Souza W (2014). Extracellular vesicles shed by *Trypanosoma cruzi* are linked to small RNA pathways, life cycle regulation and susceptibility to infection of mammalian cells. *Parasitology Research* **113**: 285–304. DOI 10.1007/s00436-013-3655-1.

Hsiung F, Ramirez-Weber FA, Iwaki DD, Kornberg TB (2005). Dependence of *Drosophila* wing imaginal disc cytonemes on Decapentaplegic. *Nature* **437**: 560–563.

Kornberg TB, Roy S (2014). Cytonemes as specialized signaling filopodia. *Development* **141**: 729–736.

Labhart P, Koller T (1981). Electron microscope specimen preparation of rat liver chromatin by a modified Miller spreading technique. *European Journal of Cell Biology* **24**: 309–316.

Mucci J, Lantos AB, Buscaglia AA, Leguizamón MS, Campetella O (2017). The *Trypanosoma cruzi* surface, a nanoscale patchwork quilt. *Trends in Parasitology* **33**: 102–112. DOI 10.1016/j.pt.2016.10.004.

Olmos-Ortiz LM, Barajas-Mendiola MA, Barrios-Rodiles M, Castellano LE, Arias-Negrete S, Avila EE, Cuéllar-Mata P (2017). *Trichomonas vaginalis* exosome-like vesicles modify the cytokine profile and reduce inflammation in parasite-infected mice. *Parasite Immunology* **39**: e12426. DOI 10.1111/pim.12426.

Rice WL, Van Hoek AN, Paunescu TG, Huynh C, Goetze B, Singh B, Scipioni L, Stern LA, Brown D (2013). High resolution helium ion scanning microscopy of the rat kidney. *PLoS One* **8**: e57051. DOI 10.1371/journal.pone.0057051.

Sant'Anna C, Campanati L, Gadelha C, Lourenço D, Labati-Terra L, Bittencourt-Silvestre J, Benchimol M, Cunha-e-Silva NL, De Souza W (2005). Improvement on the visualization of cytoskeletal structures of protozoan parasites using high-resolution field emission scanning electron microscopy (FESEM). *Histochemistry and Cell Biology* **124**: 87–95. DOI 10.1007/s00418-005-0786-1.

Szempruch AJ, Sykes SE, Kieft R, Dennison L, Becker AC, Gartrell A, Martin WJ, Nakayasu ES, Almeida IC, Hajduk SL, Harrington JM (2016). Extracellular vesicles from *Trypanosoma brucei* mediate virulence factor transfer and cause host anemia. *Cell* **164**: 246–257. DOI 10.1016/j.cell.2015.11.051.

Twu O, de Miguel N, Lustig G, Stevens GC, Vashisht AA, Wohlschlegel JA, Johnson PJ (2013). *Trichomonas vaginalis* exosomes deliver cargo to host cells and mediate host-parasite interactions. *PLoS Pathogens* **9**: e1003482. DOI 10.1371/journal.ppat.1003482.

Umaer K, Bush PJ, Bangs JD (2018). Rab11 mediates selective recycling and endocytic trafficking in *Trypanosoma brucei*. *Traffic* **19**: 406–420. DOI 10.1111/tra.12565.

Yamashita YM, Inaba M, Buszczak M (2018). Specialized intercellular communications via cytonemes and nanotubes. *Annual Review of Cell and Developmental Biology* **34**: 59–84. DOI 10.1146/annurev-cellbio-100617-062932.

Wang X, Gerdes HH (2015). Transfer of mitochondria via tunneling nanotubes rescues apoptotic PC12 cells. *Cell Death and Differentiation* **22**: 1181–1191.

Witwer KW, Théry C (2019). Extracellular vesicles or exosomes? On primacy, precision, and popularity influencing a choice of nomenclature. *Journal of Extracellular Vesicles* **8**: 1648167. DOI 10.1080/20013078.2019.1648167.